ResearchGate

See discussions, stats, and author profiles for this publication at: http://www.researchgate.net/publication/275558442

Design of a vibration isolation system using eddy current damper

ARTICLE *in* ARCHIVE PROCEEDINGS OF THE INSTITUTION OF MECHANICAL ENGINEERS PART C JOURNAL OF MECHANICAL ENGINEERING SCIENCE 1989-1996 (VOLS 203-210) · MARCH 2013

Impact Factor: 0.56 · DOI: 10.1177/0954406213489408

READS

8

3 AUTHORS, INCLUDING:

Bishakh Bhattacharya

Indian Institute of Technology Kanpur

63 PUBLICATIONS **157** CITATIONS

SEE PROFILE

Available from: Bishakh Bhattacharya
Retrieved on: 28 September 2015

Proceedings of the Institution of Mechanical Engineers, Part C: Journal of Mechanical Engineering Science
http://pic.sagepub.com/

Design of a Vibration Isolation System using Eddy Current Damper

Partha Paul, Chetan Ingale and Bishakh Bhattacharya

Proceedings of the Institution of Mechanical Engineers, Part C: Journal of Mechanical Engineering Science published online 10 May 2013
DOI: 10.1177/0954406213489408

The online version of this article can be found at:
http://pic.sagepub.com/content/early/2013/05/10/0954406213489408

Published by:
SAGE
http://www.sagepublications.com

On behalf of:
Institution of Mechanical Engineers

Additional services and information for *Proceedings of the Institution of Mechanical Engineers, Part C: Journal of Mechanical Engineering Science* can be found at:

Email Alerts: http://pic.sagepub.com/cgi/alerts

Subscriptions: http://pic.sagepub.com/subscriptions

Reprints: http://www.sagepub.com/journalsReprints.nav

Permissions: http://www.sagepub.com/journalsPermissions.nav

>> OnlineFirst Version of Record - May 10, 2013

What is This?

Downloaded from pic.sagepub.com at INDIAN INST TECH KANPUR on May 31, 2013

Original Article

Institution of MECHANICAL ENGINEERS
Journal of MECHANICAL ENGINEERING SCIENCE

Proc IMechE Part C:
J Mechanical Engineering Science
0(0) 1–12
© IMechE 2013
Reprints and permissions:
sagepub.co.uk/journalsPermissions.nav
DOI: 10.1177/0954406213489408
pic.sagepub.com
SAGE

Design of a vibration isolation system using eddy current damper

Partha Paul, Chetan Ingale and Bishakh Bhattacharya

Abstract

This article aims at modeling, analysis and design of a passive vibration isolation system using a magnetic damper with high efficiency and compactness. The experimental set-up was developed for a single degree-of-freedom vibration isolation system, where the damper consists of two elements: an outer stationary conducting tube made up of copper and a moving core made up of an array of three ring-shaped neodymium magnets of Nd–Fe–B alloy separated by four block cylinders made of mild steel that are fixed to a steel rod. The generation of eddy currents in the conductor and its resistance causes the mechanical vibration to dissipate heat energy. The vibration response of the system is obtained starting from a low-frequency range. The proposed magnetic damper achieves a maximum transmissibility value less than two for a natural frequency that is less than 10 Hz and the excitations at higher frequencies are successfully isolated. Numerical and experimental studies were carried out for a range of system parameters which show that isolators based on magnetic damping could be very effective for passive vibration isolation. Further, a theoretical model for an active isolation system is proposed in order to reduce the transmissibility at resonance. It is envisaged that the combined active–passive eddy current damper could be effectively used for vibration isolation.

Keywords

Passive and active vibration isolation, eddy current damping, electromagnetic vibration isolator, direct output feedback control

Date received: 7 December 2012; accepted: 20 March 2013

Introduction

Vibration isolation is a way of reducing the transmission of a dynamic excitation force (or motion) from a mechanical system to a supporting surface.[1] It generally involves the insertion of a layer of resilient material between the source of vibration and the system to be isolated. The effectiveness of a vibration isolator is generally measured in terms of the maximum transmissibility, cut-off frequency and cut-off rate (Figure 1). The chief objectives to be fulfilled while designing an effective vibration isolator are[2]

(a) low-resonance frequency (so that the damper isolates the system for a broad frequency range);
(b) low amplitude of vibration at resonance and
(c) steep slope of the transmittability curve (high attenuation at higher frequency).

Vibration isolators are broadly subdivided into two groups based on the requirement of external power supply: passive and active isolators. Passive isolators commonly include passive elements such as metallic or non-metallic springs, viscous and friction-based dampers, elastodamping materials and pneumatic/hydraulic elements. On the other hand, active damping is less common in industrial applications and includes isolators such as active hydraulic network, electromagnetic damper, electromagneto rheological fluids, sensors and control systems.

In this article, we will discuss about the design of a new passive vibration isolation system based on the electromagnetic effect. We will compare the theoretical and experimental results for this passive system and study the effect on the displacement transmissibility of the system. Next, we will introduce an active isolation system into the theoretical model to further reduce the transmissibility of the system.

Energy dissipation characteristics of a damper based on eddy current generation allow many applications in vibration control of machines and structural vibration suppression. Eddy current-based

Department of Mechanical Engineering, IIT Kanpur, Kanpur

Corresponding author:
Partha Paul, Department of Mechanical Engineering, IIT Kanpur, Kanpur, India.
Email: contactpauljunior@gmail.com

Downloaded from pic.sagepub.com at INDIAN INST TECH KANPUR on May 31, 2013

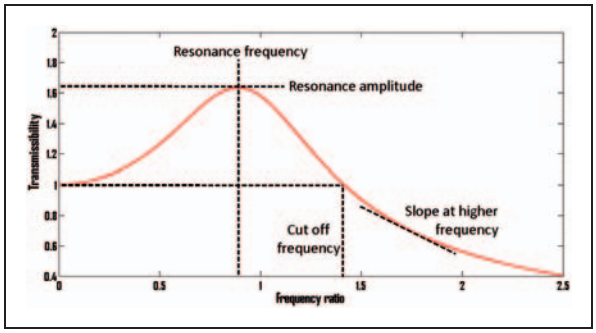

Figure 1. Salient features of a vibration isolator.

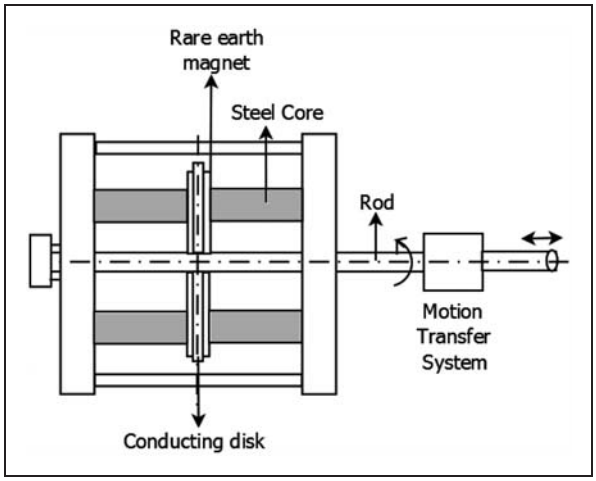

Figure 2. Schematic diagram of a magnetic hybrid damper.[7]

dampers have been known for decades and their applications are thoroughly investigated.[3] In an eddy current braking system, Cadwell[4] examined the effect of magnetic damping on an aluminum plate that moved between the poles of a horseshoe electromagnet and developed a model to find the braking force using an air track for experimental analysis. Wiederick et al.[5] proposed a simple theory and experiment of magnetic braking in a thin metallic strip. An eddy current is induced by spinning a thin aluminum disc between the poles of an electromagnet and the accuracy is validated by a theoretical model.

Control techniques have been used to adjust the damping force obtained from traditional damping systems. Lee and Park[6] designed an optimal controller for an eddy current brake to minimize the stopping time of a disc in an automobile. It worked well in the high-speed range because the damping force is directly proportional to the angular speed. A semi-active damping system based on hybrid electromagnets is available in the literature,[7] the schematic of which is elucidated in Figure 2. Due to relative motion, a damping torque is generated in the conductive disc. This model uses the magnetization and demagnetization effects to control the damping force.

Zheng et al.[8] used a magnetic damper to suppress the vibration of a beam. It includes both an active and a passive method. An electromagnet is attached to the clamped boundary and a permanent magnet is attached to the beam. Current is passed through the coil whenever a damping force is required. Sodano et al.[9] studied the model of an eddy current damper for vibration suppression of a beam. The model consists of a beam with a conducting sheet and a permanent magnet at a small distance. The system has been shown to increase the damping ratio by at least two orders of magnitude and provide a damping force that is sufficient to suppress the vibration of the beam. Karnopp[10] introduced the concept of an electromechanical damper for a vehicle suspension system. It consists of moving coils of copper wire and permanent magnets. This actuator provides better damping for frequencies encountered in road vehicle suspension.

Kobayashi and Aida[11] modeled a vibration absorber using an eddy current damper to reduce the vibration generated by pipes in industrial buildings. It consists of a mass and a damper. Experiments were performed on a 2.4 m pipe which showed that the first bending mode of the pipe was reduced by eight to ten times with displacements ranging from 0.4 to 4 mm.

Teshima et al.[12] studied the effect of eddy current dampers on vibration response in superconducting levitation. Damping was reported to be improved by two orders of magnitude by the insertion of eddy current dampers into the gap between the superconductor and the magnet. Melt-processed YBaCuO superconductor was used for the study. Ebrahimi et al.[13] developed an experimental set-up for an eddy current damper. The damper configuration consists of a copper tube as a conductor and an array of permanent magnets and iron pole pieces as the moving elements.

Ebrahimi et al.[14] analyzed a passive eddy current damper using different configurations of permanent magnets by using magnets magnetized in axial and radial directions. A finite element analysis was carried out to find the optimum magnetic flux for different configurations. Wang et al.[15] analyzed and optimized the design of an axially magnetized tubular permanent magnet. The analytical modeling is subsequently validated by finite element analysis. This gives a basis for designing an optimized model of an eddy current isolator.

Damper assembly model

For magnetic dampers it is known that the coefficient of damping is proportional to the conductivity of the conductor and the square of flux density. Hence, the damper assembly is designed in such a way that it has minimum flux leakage and the copper body is chosen as the conductor to facilitate eddy current generation. Figure 3 shows the schematic diagram of the damper assembly. It consists of an outer stationary tube made

Downloaded from pic.sagepub.com at INDIAN INST TECH KANPUR on May 31, 2013

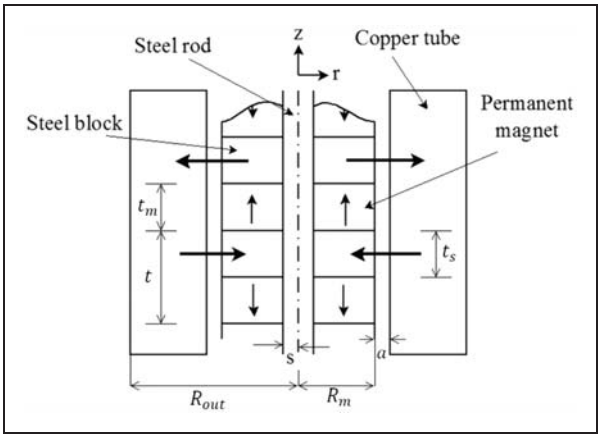

Figure 3. Schematic diagram of the damper assembly.

of copper, three permanent ring-shaped magnets made of neodymium, cylindrical blocks of steel and a screwed steel rod. The permanent magnets are axially magnetized and their direction of magnetization is also shown in the figure. The horizontal bold arrows show the direction of magnetic flux through the steel block. The magnets and steel blocks are fixed tightly to the supporting steel rod and the air gap is kept very small to minimize the flux leakage.

Relative movement between the magnets and the conductor generates an eddy current and produces a repulsive force proportional to relative velocity between them. Due to the generation of eddy currents and the resistance of the conductor, the mechanical energy due to vibration gets dissipated through Joule heating in the conductor. The parameters and variables in Figure 3 are given in Table 1.

Table 1. Specifications of the magnetic damper assembly used.

Outer diameter of the magnet ($2R_m$)	28 mm
Inner diameter of the magnet ($2r_m$)	10 mm
Thickness of the magnet (t_m)	12.5 mm
Outer diameter of the steel block ($2R_s$)	28 mm
Inner diameter of the steel block ($2r_s$)	10 mm
Thickness of the steel block (t_s)	10 mm
Diameter of the steel rod ($2s$)	10 mm
Outer diameter of the conductor ($2R_{out}$)	75 mm
Inner diameter of the conductor ($2R_{in}$)	29 mm
Length (l)	85 mm
Conductivity of copper (σ)	5.96×10^7 S m^{-1}
Air gap (a)	0.5 mm
Magnetization constant (M)	10^6 A m^{-1}
Mass to be isolated (m)	2.02 kg
Stiffness of the spring (k)	7.4 kNm^{-1}
Natural frequency (ω_n)	9.64 Hz
Cut-off frequency	13.63 Hz
Cut-off rate (per Hz)	0.125
Damping co-efficient per steel block	33.28 Ns m^{-1}
Total damping co-efficient (c)	99.84 Ns m^{-1}
Critical damping (c_c)	244.62 Ns m^{-1}
Damping ratio (ξ)	0.408

Methodology

Governing equation of motion

The vibration isolator is modeled as a single degree-of-freedom system consisting of a spring and dashpot in parallel (Figure 5).

$$m\ddot{x} + c\dot{x} + kx = c\dot{y} + ky \tag{1}$$

where m is the isolator mass, x is the vibrational displacement of the mass to be isolated, c is the co-efficient of damping of the system, k is the spring constant of the system and $\boldsymbol{y}$ is the base excitation (displacement).

Analytic damping coefficient estimation

The damping force per steel block, assuming a constant magnetic flux density is given by the Lorentz force law as

$$F = \int_{\Gamma} \sigma(v \times B) \times B \, \mathrm{d}\Gamma \tag{2}$$

where σ is the conductivity of copper, v is the relative velocity of the conductor with respect to the magnetic field and B is the magnetic flux density.

For the calculation of magnetic flux density (B), the current model proposed by Craik[16] is used. Since the movement of copper cylinder is along the z-direction, the eddy current generation depends on the radial component of magnetic flux density (B_r). The radial component of magnetic flux density at a distance (r, z) from the geometric center is computed using the relation (10) (see Appendix 1) and $K(k)$ and $E(k)$; the complete elliptic integrals of the first and second kind, the parameter 'k' being a function of R_m (outer radius of magnet), t_m (thickness of the magnet), s (radius of the steel rod), r and z (symbols shown in Figure 3).

Figure 4 shows the schematic view of the design of the permanent magnets. The radial magnetic flux density (B_r) through each steel block is twice as produced by one magnet. Hence, the total radial component of the magnetic flux density (B_r) per steel block is given by

$$B_r = 2\left(B_r(r,z)|_{R_m,\,t_m} - B_r(r,z)|_{s,\,t_m}\right) \tag{3}$$

Now, using equations (1) to (3), the damping force (F_z) per steel block in the z-direction is given by

$$F_z = -\sigma(t - t_m)v \int_0^{2\pi} \int_{R_{in}}^{R_{out}} r B_r^2(r, z_0) \mathrm{d}r \, \mathrm{d}\theta \tag{4}$$

Downloaded from pic.sagepub.com at INDIAN INST TECH KANPUR on May 31, 2013

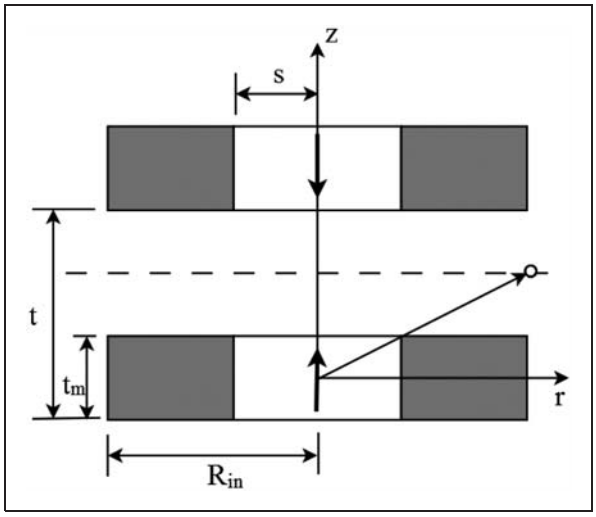

Figure 4. Schematic view of the two permanent magnets.

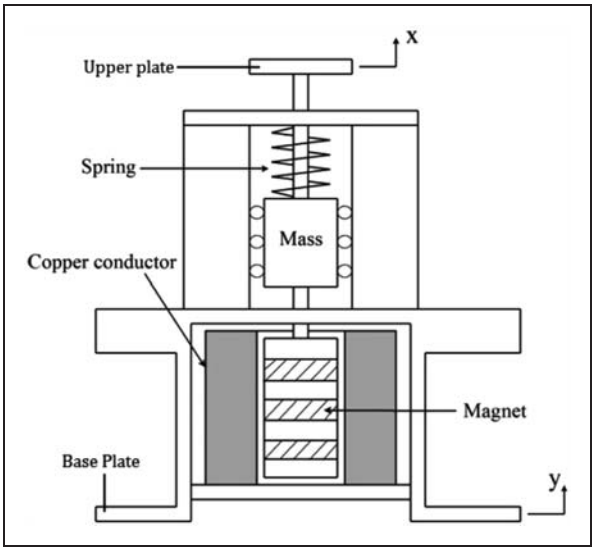

Figure 5. Schematic diagram of the vibration isolation device.

Hence from equation (4) coefficient of damping (C) is given by

$$C = -\sigma(t - t_m)\int_0^{2\pi}\int_{R_{in}}^{R_{out}} rB_r^2(r, z_0)\mathrm{d}r\,\mathrm{d}\theta \tag{5}$$

Equation (5) is computed in MATLAB to calculate the coefficient of damping for the given dimension of damper assembly given in Table 1 and later compared with the experimental results.

One of the parameters used for measuring the effectiveness of a vibration isolator is the maximum transmissibility. Under steady-state conditions, both force and displacement transmissibilities are the same. (Henceforth, the terms displacement transmissibility and transmissibility are used interchangeably and mean the same thing: the displacement transmissibility.)

The transmissibility (T) for the given single degree-of-freedom system is given by

$$T = \left|\frac{X}{Y}\right| = \frac{\sqrt{1 + (2\xi r)^2}}{\sqrt{(1 - r^2)^2 + (2\xi r)^2}} \tag{6}$$

where $\boldsymbol{r}$ is the frequency ratio and ξ is the damping ratio.

The complete derivation is shown in Appendix 1.

It may be noted that for $r < \sqrt{2}$, the transmissibility is greater than 1 which indicates the amplification region; whereas for $r > \sqrt{2}$, transmissibility is less than 1 which indicates the isolation region. The frequency corresponding to $r = \sqrt{2}$ is known as the cut-off frequency. For a good isolator, the cut-off frequency is designed to be kept well below the excitation range.

Experimental set-up

Figure 5 shows the proposed passive vibration isolation system for the single degree-of-freedom system. As shown in Figure 6(a) and (b), it consists of two C-channels, a hollow copper cylinder, a base plate, a mass to be isolated, a spring, upper plate, threaded rod, two columns to support the needle roller bearing and the damper assembly. All the parts are made of mild steel. Four needle bearings are provided to prevent any lateral movement of the isolated mass. An accelerometer (of Brüel and Kjaer of type 4384) is mounted on the upper plate. The damper assembly consists of a hollow copper cylinder and an array of magnets and mild steel cylindrical blocks. These magnets and steel blocks are screwed tightly to the steel rod. The permanent magnets are axially magnetized and made up of Nd–Fe–B alloy.

Figure 7 shows the experimental set-up for the passive vibration isolator. The whole set-up is mounted on a shaker table at the base of C-channels so that there is no slip. The accelerometer is mounted on the upper plate to measure the response of the isolated mass (m). After mounting the isolation device on the shaker table, a harmonic excitation is given in the range of 5–30 Hz with a step up frequency of 0.1 Hz via a shaker (Model 150 VP-T). The amplitude of the shaker table (Y) is kept constant at 6.35×10^{-4} m. Experiments are carried out to study the transmissibility of the isolator.

As a result of harmonic base excitation, there is a relative movement between the copper conductor and the permanent magnets. Due to this relative movement, eddy currents are developed in the copper cylinder. The current circulates inside the conductor generating a magnetic field with a polarity opposite to the applied magnetic field. This current produces a repulsive force which is proportional to the relative velocity between the copper conductor and the magnets.

Figure 8 shows the detailed flow chart of the experimental set-up.

Downloaded from pic.sagepub.com at INDIAN INST TECH KANPUR on May 31, 2013

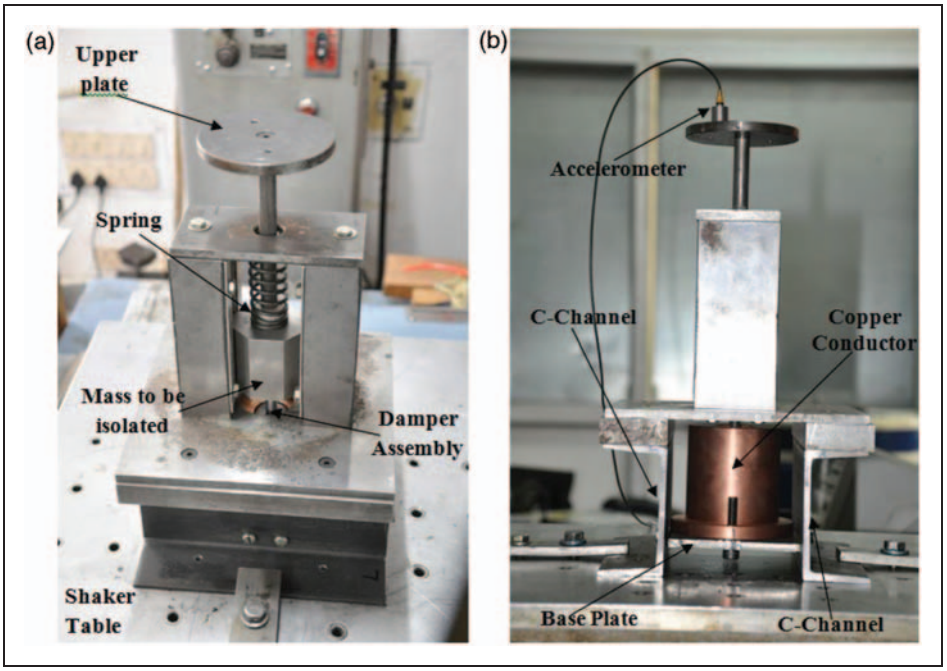

Figure 6. (a and b): experimental set-up of the passive vibration isolator using a magnetic damper.

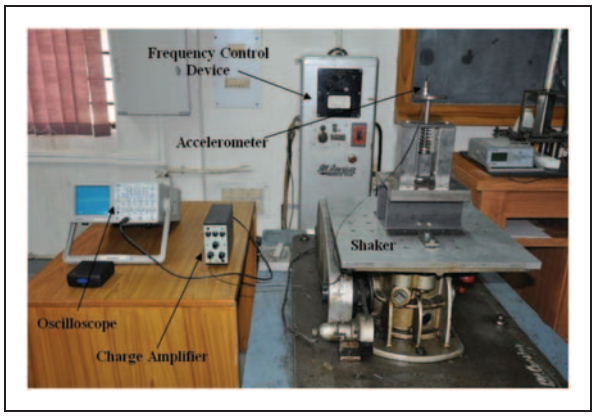

Figure 7. Complete experimental set-up for the passive vibration isolator.

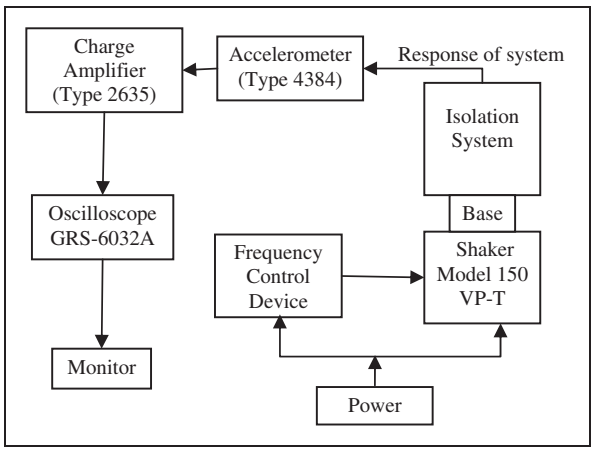

Figure 8. Flowchart of the experimental set-up.

Optimization of steel block thickness

The size of the cylindrical steel block is calculated by considering the dimension of a commercially available magnet. Since from equation (5), the coefficient of damping (C) is a function of the thickness of the steel block (t_s) (as shown in Figure 9), it is designed to obtain maximum damping. The maximum magnetic flux is obtained at t_m/t equal to 0.55. Equation (5) for the damping coefficient is computed for various thickness of steel block. Figure 9 shows the variation of coefficient of damping with respect to steel block thickness (t_s). It is observed that the coefficient of damping is maximum when the thickness of the steel block is close to 10 mm.

Results

The experiments were carried out for a base vibration amplitude of 0.625 mm (peak-to-peak) and for a frequency range of 5–30 Hz.

Dynamic analysis of the platform

This is necessary to ensure effective decoupling of the isolator resonating frequency from the natural frequency of the platform. It is also required to ensure that the supporting column does not interfere with the movement of the magnetic block during vibration. To find the fundamental frequency of the structure, a modal analysis of the platform was performed using ABAQUS as shown in Figure 10.

It is found that the fundamental frequency of the structure is 236.64 Hz. Hence, the excitation

Downloaded from pic.sagepub.com at INDIAN INST TECH KANPUR on May 31, 2013

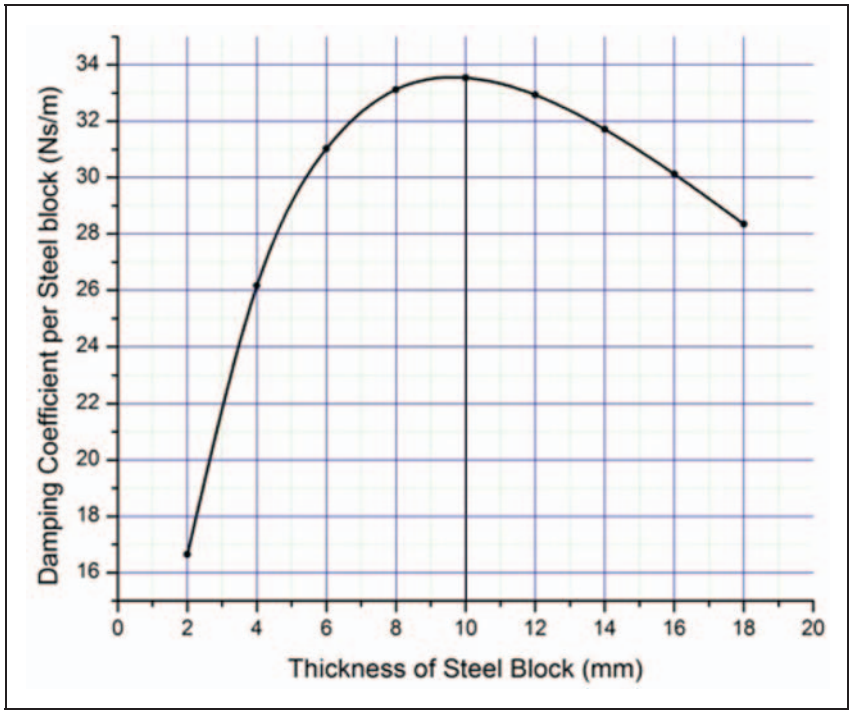

Figure 9. Damping coefficient (C) vs. steel block's thickness.

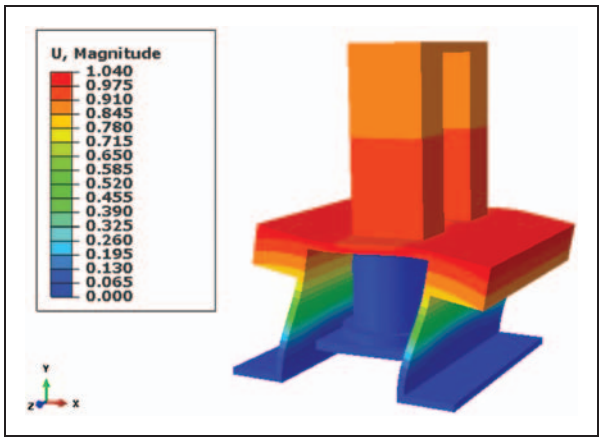

Figure 10. Mode shape at a frequency of 236.64 Hz.

frequency range is kept below the fundamental frequency. The other frequencies at which the mode numbers are obtained are 532.68 Hz, 815.46 Hz, 1027.20 Hz and 1044.40 Hz. The frequency resolution is 0.01 Hz.

Response of isolator without damper

Figure 11 shows the transmissibility curve for the isolator without magnetic damper having a mass of 1.643 kg and a spring stiffness of 7.4 kNm^{-1}.

The maximum displacement transmissibility is found to be 15.8 at a frequency of 9.9 Hz. The cut-off frequency is 15.5 Hz with a cut-off rate 0.161 Hz^{-1}.

Response of isolator using magnetic damper

Figure 12 shows the transmissibility with an isolator of mass of 2.02 kg, spring stiffness as 7.4 kNm^{-1} and the coefficient of damping as 99.84 Ns m^{-1}. The maximum displacement transmissibility is found to be close to 1.73 at a frequency of 9.9 Hz. The cut-off frequency is 14.6 Hz with the cut-off rate 0.103 Hz^{-1}. The quality factor of the system is 1.995. This shows that by using magnetic damper the transmissibility is decreased 9 times at a resonating frequency of 9.9 Hz.

Comparison of performance in time domain

Figure 13 shows the displacement on a time scale for harmonic excitation at the resonating frequency. The peak-to-peak amplitude of the base is 0.635 mm. The maximum amplitude of the system originally is 10.03 mm and comes down to 1.09 mm after adding the eddy current damper.

A comparison of the transmittability with and without the use of magnetic damper is shown in Figure 14. The experimental results confirm the analytical model which predicts the damping ratio to be 0.408, maximum transmissibility to be 1.63 and cut-off frequency 13.6 Hz with a cut-off rate of 0.125.

Variation in isolator mass

The effect of variation of the isolated mass (m) on the response of the isolator and sensitivity of the isolation parameters with respect to the change of mass compared with a reference mass of 2.02 kg is studied

Downloaded from pic.sagepub.com at INDIAN INST TECH KANPUR on May 31, 2013

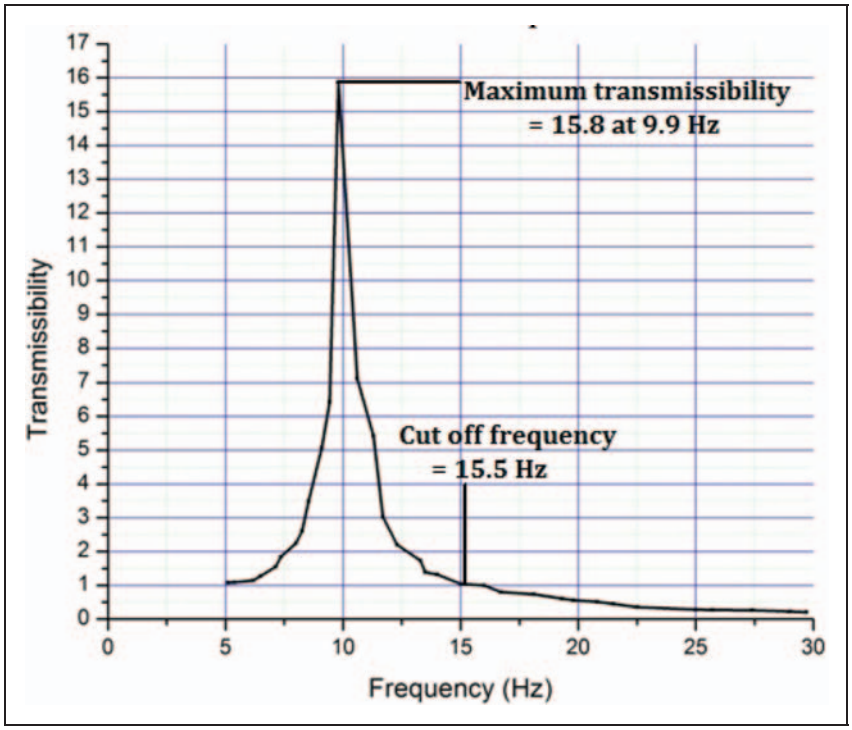

Figure 11. Transmissibility plot of the isolator without magnetic damper.

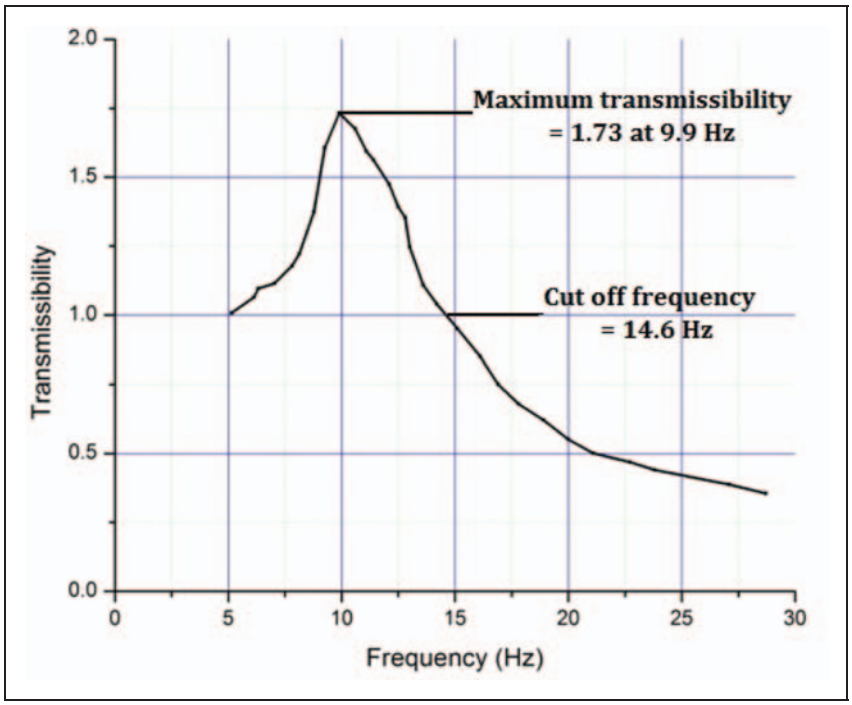

Figure 12. Transmissibility plot of the isolator with magnetic damper.

experimentally. Table 2 shows the sensitivity of the isolation parameter with respect to this change of mass. The frequency resolution of the instrument is 0.01 Hz.

The natural frequency and cut-off frequency is further reduced with the increase in the additional mass to get a broad range of isolation region.

Figure 15 shows the transmissibility curves for the isolator with different masses as shown in Table 2.

Active control of vibration isolation

Passive vibration control has a limitation that the vibration isolation can only be achieved for a fixed

Downloaded from pic.sagepub.com at INDIAN INST TECH KANPUR on May 31, 2013

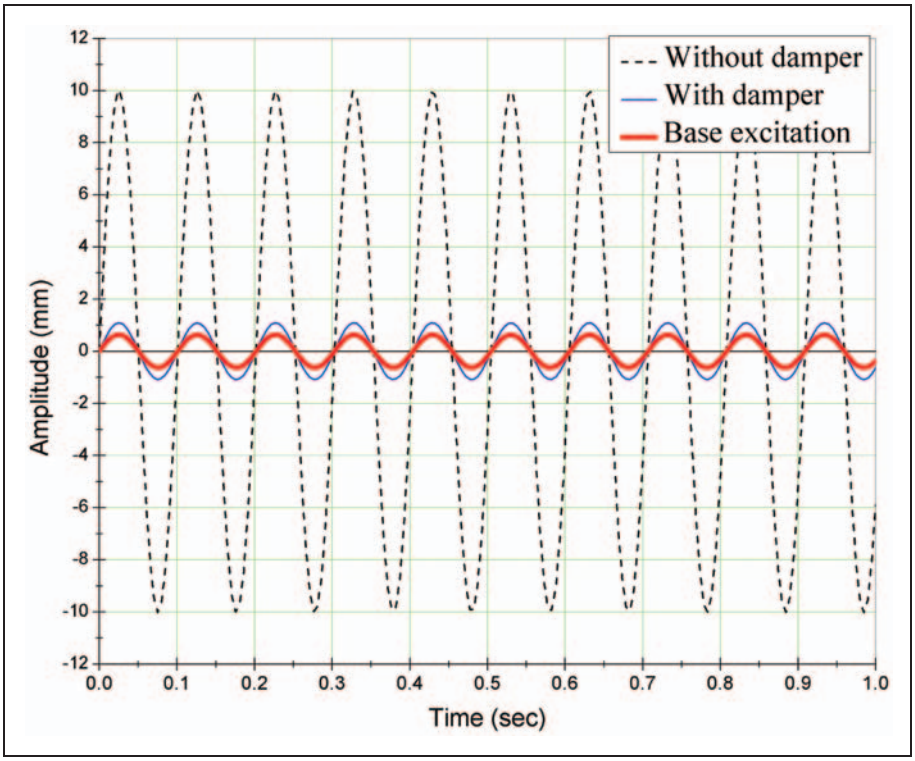

Figure 13. Displacement vs. time at resonance frequency of 9.9 Hz.

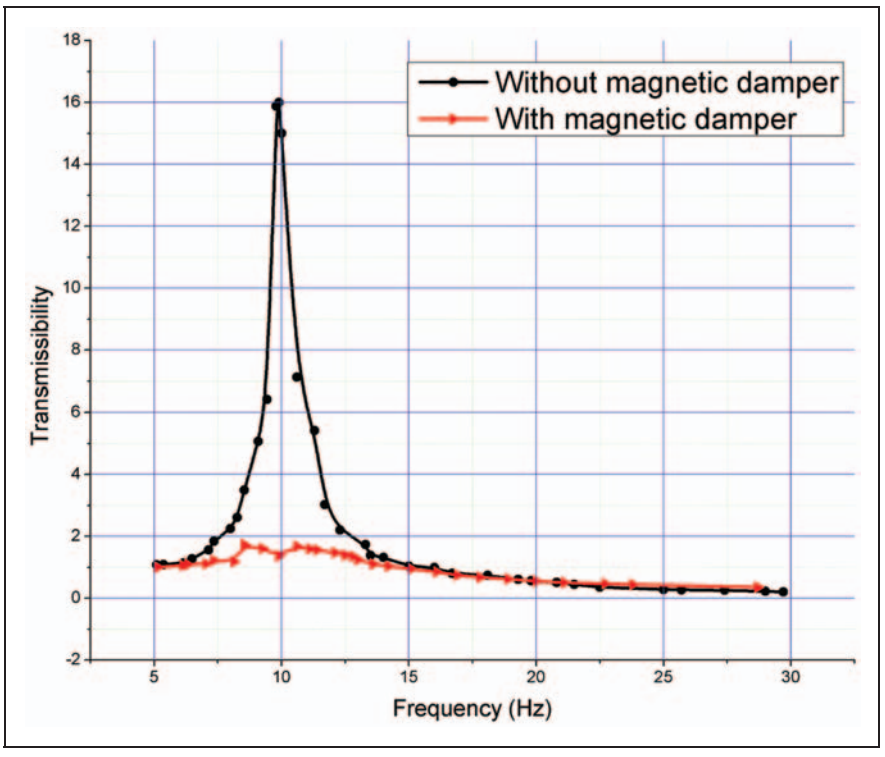

Figure 14. Comparison of transmissibility curve of isolator.

set of parameters. Active vibration isolation gives a marked advantage over passive isolation in that it can be achieved over a wide range of the system gain.

Further, as is evident from the previous section, the transmissibility is brought down to 1.73 with passive vibration isolation. This value can further be reduced by the introduction of active isolation and driving the system toward critical damping.

The method used for active isolation is the integration of direct output feedback control[17] into the

Downloaded from pic.sagepub.com at INDIAN INST TECH KANPUR on May 31, 2013

Table 2. Sensitivity of the isolation parameters for different masses.

Parameters	$m = 2.520$ kg	$m = 3.156$ kg	$m = 3.656$ kg
Transmissibility	0.257	0.164	0.021
Cut-off frequency (Hz)	0.33	0.32	0.29
Cut-off rate (Hz^{-1})	0.27	1.38	0.81

open-loop characteristics of the system. Figure 16 shows the open-loop root locus of the system obtained from its state space representation.

Direct output feedback control is achieved by controlling the feedback gain in two parts: the position gain (K_d) and the velocity gain (K_v) as seen in Figure 17.

The family of root loci for different gains gives the movement of the closed-loop poles toward the critically damped condition (point of intersection of the pole pair with the negative real axis). Then, the

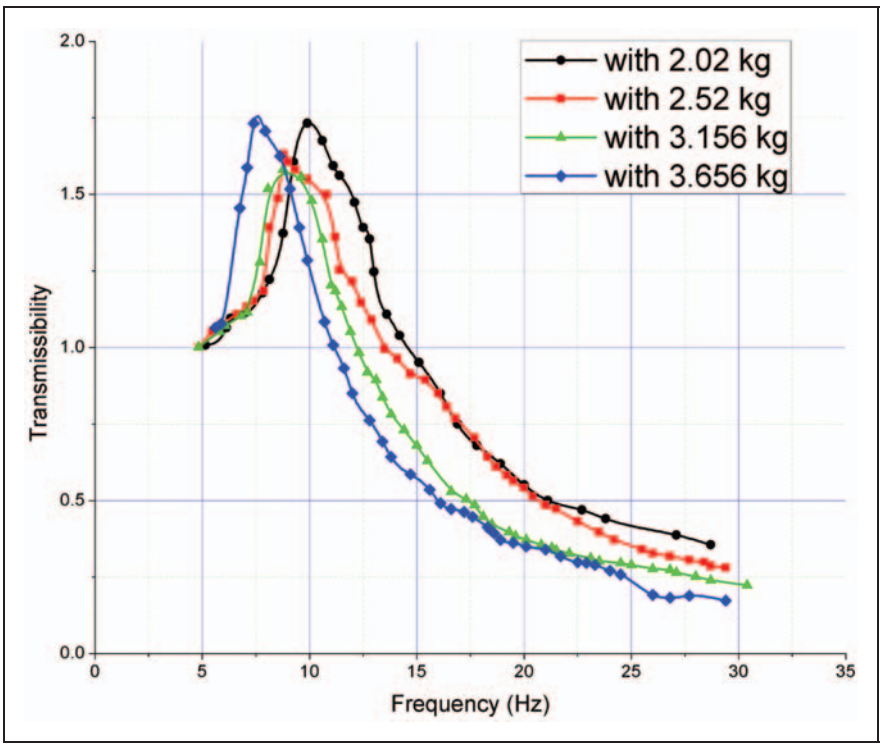

Figure 15. Effect of the variation in mass on the isolator.

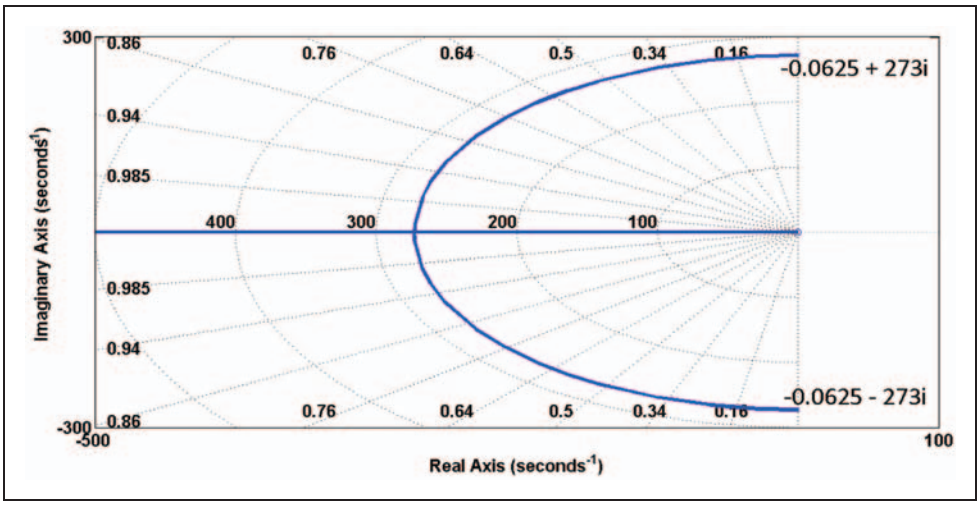

Figure 16. Open-loop root locus of the system.

Downloaded from pic.sagepub.com at INDIAN INST TECH KANPUR on May 31, 2013

closed-loop frequency and gain can be determined for the critically damped system.

Figure 18 shows the critically damped condition in the family of root loci for $K_d = 100$ and $K_v = 450$.

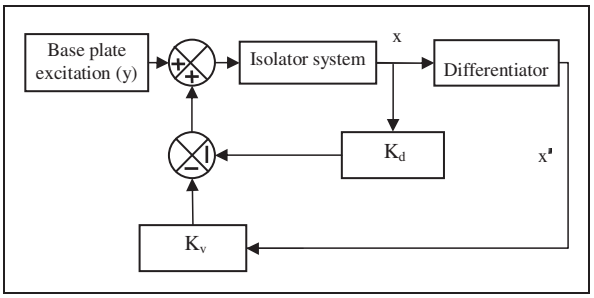

Figure 17. Block diagram showing direct output feedback control.

Figure 19 shows the critically damped condition in the family of root loci for $K_v = 100$ and $K_d = 4.5 \times 10^5$.

The difference in the two cases is the convergence of the poles to the critically damped condition. While the distance of the pole from the origin is constant in the former case (Figure 18), the real intercept of the poles remain constant in the latter case (Figure 19).

The qualitative plot for the transmissibility of the closed-loop system can be obtained by the superimposition of the plots of the vibration of the upper plate and base plate and studying the decay of the isolator mass vibration as shown in Figure 20.

This proposed active system can be integrated into the experimental set-up of the current passive isolation system to further reduce the displacement transmissibility of the isolator.

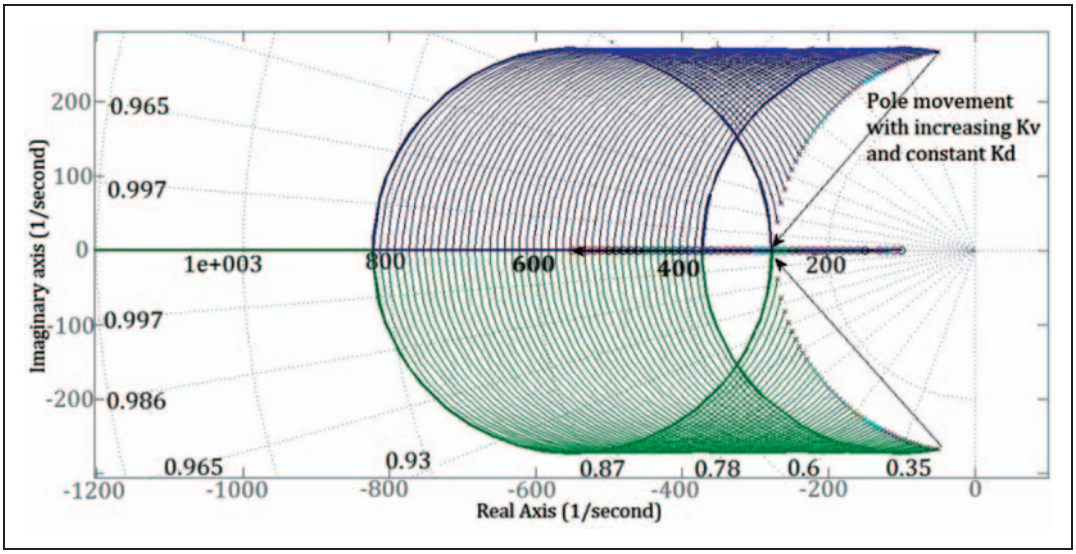

Figure 18. Closed-loop root locus of the system with constant $K_d = 100$ and variable K_v (between 100 and 450).

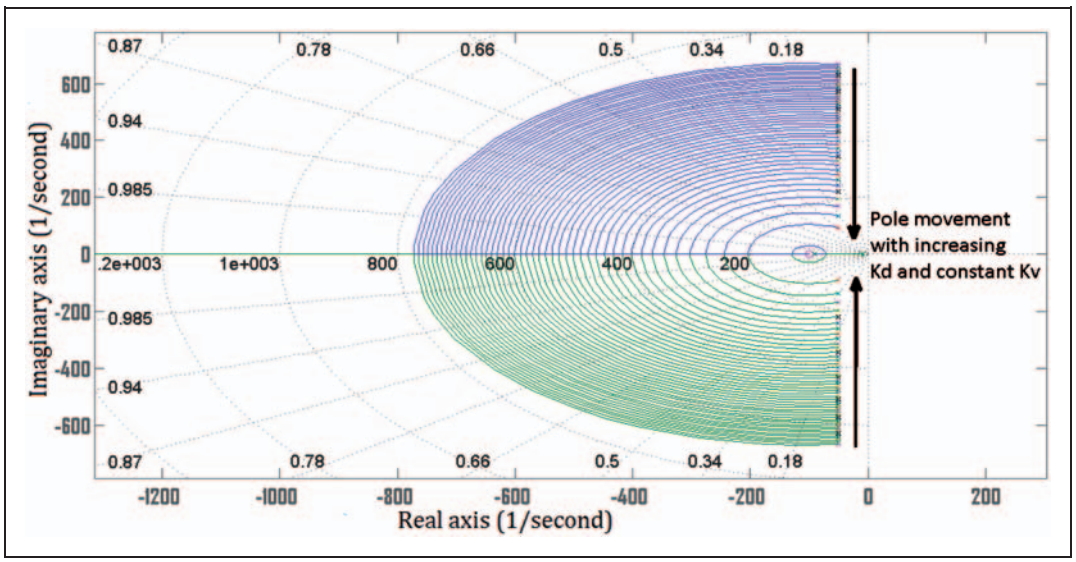

Figure 19. Closed-loop root locus of the system with constant $K_v = 100$ and variable K_d (between 100 and 4.5×10^5).

Downloaded from pic.sagepub.com at INDIAN INST TECH KANPUR on May 31, 2013

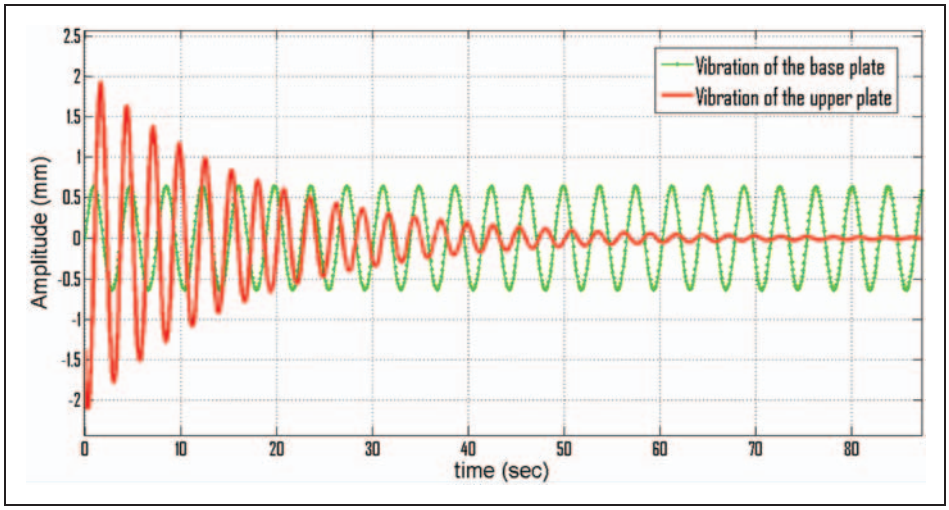

Figure 20. Qualitative plot of the transmissibility with gains $K_d = 100$ and $K_v = 100$.

Conclusion and future work

This article describes the basic design of a vibration isolation system platform based on eddy current damping. It is found that at resonance, the maximum amplitude of the displacement for the designed isolator decreases from 10.03 mm to 1.09 mm. The displacement transmissibility without the damper is 15.8 which is reduced to 1.73 after using the eddy current damper. Beyond the cut-off frequency of 14.6 Hz, the system is successfully isolated with a cut-off rate of 0.103 Hz^{-1}. Analytical results show a good matching with the experimental results in the low-frequency region.

The resonance frequency has remained unchanged because this damper does not add any additional stiffness to the system. Thus, eddy current-based passive damping system could be a very effective solution for a broad frequency range of vibration isolation.

Subsequently, a simulation is carried out for the active vibration isolation of the system using direct output feedback control to plot the closed-loop response of the system and determine the behavior of the isolator over a wider range of frequencies and gains while further reducing the transmissibility as compared to passive isolation.

The performance of an isolator can be further improved by using higher quality magnets and conductor. A different configuration in the design of damper assembly can be achieved by using magnets with different directions of magnetization. These dampers can be arranged in series or in parallel to design different types of isolators. Further, for active vibration control, the permanent magnets can be replaced by electromagnets so that the damping can be controlled in real time.

Funding

The authors gratefully acknowledge the travel support of UKIERI (UKIERI/MDeS/20120045) for disseminating the works at the University of Sheffield, Sheffield, UK.

Conflict of interest

None declared.

References

1. Rivin EI. *Passive vibration isolation*. New York: ASME Press, 2003, pp.3–6.
2. Mallik AK. *Principles of vibration control*. New Delhi: Affiliated East-West Press, 1990, pp.149–150.
3. Sodano HA and Bae JS. Eddy current damping in structures. *Shock Vib Digest* 2004; 36(6): 469–478.
4. Cadwell LH. Magnetic damping: analysis of an eddy current brake using an airtrack. *J Phys* 1996; 64: 917–923.
5. Wiederick HH, Gauthier N, Campbell DA, et al. Magnetic braking: simple theory and experiment. *Am J Phys* 1987; 55: 500–503.
6. Lee K and Park K. Optimal robust control of a contactless brake system using an eddy current. *Mechatronics* 1999; 9(6): 615–631.
7. Matsuoka T, Sunakoda K and Zeniya M. Development of magnetic damper using hybrid electromagnet. In: *12th Asia pacific vibration conference*, Sapporo, Japan, 2007.
8. Zheng H, Li M and He Z. Active and passive magnetic constrained damping treatment. *Int J Solids Struct* 2003; 40: 6767–6779.
9. Sodano HA, Bae JS, Inman DJ, et al. 2004 a. *Concept and model of eddy current damper for vibration suppression of a beam*. J Sound Vib 2005; 288: 1177–1196.
10. Karnopp D. Permanent magnet linear motors used as variable mechanical dampers for vehicle suspensions. *J Veh Syst Dyn* 1989; 18: 187–200.
11. Kobayashi H and Aida S. Development of a houde damper using magnetic damping. In: *Vibration isolation, acoustics and damping in mechanical systems ASME*. vol. 62, 1993, pp.25–29.
12. Teshima H, Tanaka M, Miyamoto K, et al. Effect of eddy current dampers on the vibration properties in superconducting levitation using melt-processed **YBaCuO** bulk superconductors. *Physica C* 1997; 274: 17–23.
13. Ebrahimi B, Khamesee MB and Golnaraghi F. A novel eddy current damper: theory and experiment. *J Phys D: Appl Phys* 2009; 42(075001): 1–6.

Downloaded from pic.sagepub.com at INDIAN INST TECH KANPUR on May 31, 2013

14. Ebrahimi B, Khamesee MB and Golnaraghi F. Permanent magnet configuration in design of and eddy current damper. *Microsyst Technol* 2008; 16: 19–24.
15. Wang J, David H and Jewell GW. Analysis and design optimization of an improved axially magnetized tabular permanent magnet machine. *IEEE Trans Energy Conver* 2004; 19(2): 289–295.
16. Craik DJ. *Magnetism principles and applications*. Wiley-Blackwell, 1995, pp.334–336.
17. Meirovitch L. *Dynamics and control of structures*. New York: John Wiley & Sons, 1982, p.357.

Appendix 1

Analytical damping coefficient estimation

The eddy currents produced create a magnetic flux in such a way that it opposes the external magnetic field. This gives a damping force in z-direction. The resulting damping force (F) per steel block is given by the Lorentz force law as

$$F = \oint JxBd\Gamma \tag{7}$$

where

Γ is the conductor's volume, J is the induced current density and B is the magnetic flux density.

By assuming a constant magnetic flux density, the induced current density (J) is calculated as

$$J = \sigma(v \times B) \tag{8}$$

where

J is the current density,

σ is the conductivity of copper and

v is the relative velocity of the conductor with respect to the magnetic field.

There are many methods for calculating the magnetic flux density of a permanent magnet. Here for the calculation of magnetic flux density, the current model proposed by Craik[16] is used. It is an accurate model with reasonable complexity. Since the movement of copper cylinder is along the z-direction, the eddy current generation depends on the radial component of magnetic flux density (B_r). The radial component of magnetic flux density at distance (r, zr, z) from the geometric center is given by

$$B_r(r,z)|_{R_m,t_m} = \frac{\mu_0 I}{2\pi t_m}\int_{-t_m/2}^{t_m/2} \frac{(z-z')}{r\left[(R_m+r)^2+(z-z')^2\right]^{1/2}} X \times \left[-K(k)\frac{R_m^2+r^2+(z-z')^2}{(R_m-r)^2+(z-z')^2}E(k)\right]dz' \tag{9}$$

where t_m is the permanent magnet's thickness, R_m is the permanent magnet's radius, μ_0 is the permeability of free space, $I = M\ t_m$, equivalent current, M is the magnetization constant of permanent magnet and $K(k)$ is the complete elliptic integral of the first kind.

$$K(k) = \int_0^{\pi/2} \frac{d\theta}{\sqrt{1-k^2\sin^2\theta}} \tag{10}$$

$E(k)$ is the complete elliptic integral of the second kind

$$E(k) = \int_0^{\pi/2} \sqrt{1-k^2\sin^2\theta}\, d\theta \tag{11}$$

and the parameter k is given by

$$k^2 = \frac{4R_m r}{(R_m+r)^2+(z-z')^2} \tag{12}$$

The radial magnetic flux density (B_r) through each steel block is twice as produced by one magnet (see Figure 4). Hence total radial component of the magnetic flux (B_r) density per steel block is given by

$$B_r = 2\left(B_r(r,z)|_{R_m,t_m} - B_r(r,z)|_{s,t_m}\right) \tag{13}$$

Now using equations (7) to (13), the damping force (F_z) per steel block in z-direction is given by

$$F_z = \sigma(t-t_m)v\int_0^{2\pi}\int_{R_{in}}^{R_{out}} rB_r^2(r,z_0)dr\,d\theta \tag{14}$$

Hence from equation (14) coefficient of damping (C) is given by

$$C = -\sigma(t-t_m)\int_0^{2\pi}\int_{R_{in}}^{R_{out}} rB_r^2(r,z_0)dr\,d\theta \tag{15}$$

Force transmissibility, one of the characteristics that defines the effectiveness of a vibration isolator, is defined as the ratio of the amplitude of the force transmitted to that of exciting force. Displacement transmissibility is defined as the ratio of amplitude of mass which is isolated (X) to the amplitude of the base excitation (Y). For steady-state condition both are the same.

$$\omega_n = \sqrt{\frac{k}{m}}, \quad r = \frac{\omega}{\omega_n}, \quad \xi = \frac{c}{c_c} \quad \text{and} \quad c_c = 2\sqrt{mk} \tag{16}$$

where ω_n is the natural frequency in rad s^{-1}, r is the frequency ratio, c_c is the critical damping coefficient and ξ is the damping ratio.

Downloaded from pic.sagepub.com at INDIAN INST TECH KANPUR on May 31, 2013